Organic Materials in Optoelectronic Applications: Physical Processes and Active Devices

ACADEMIC AND RESEARCH STAFF

Professor Vladimir Bulović

GRADUATE STUDENTS

Seth Coe, John Ho, Sung Hoon Kim, Eko Lisuwandi, Conor Madigan, Debbie Mascaro, Aimee Rose, Jonathan Tischler

UNDERGRADUATE STUDENTS

Criswell Choi, Kim Falinski, Mimi Gupta, Nathan Lovell, Sharon Voshell

Laboratory of Organic Optoelectronics - Research Themes

Our group studies physical properties of organic thin films, structures, and devices. Our fundamental findings are applied to the development of optoelectronic, electronic, and photonic organic devices of nano-scale thickness, including visible LEDs, lasers, solar cells, photodetectors, transistors, memory cells, and chemical sensors. In addition to working on small-molecular-weight van-der-Waals-bonded organic thin films, we also examine hybrid organic/inorganic structures, polymer solids, and self-assembled materials. Our work tends towards the nano-scale where through development of new patterning and materials growth techniques we aim to reduce the size of active organic layers from the present nano-scale thickness of organic thin films to that of single molecules. Our ultimate goal is to probe functionality of single molecules or polymer strands and to utilize molecular, polymer, or inorganic/organic hybrid assemblies in nano-scale devices and integrated systems.

Integrated Materials Growth System

SPONSOR

Defense University Research Instrumentation Program (DURIP) - Air Force Office of Scientific Research

NSF Center for Materials Science and Engineering SEED Grant

PROJECT STAFF

Seth Coe, Conor Madigan, Debbie Mascaro, Sung Hoon Kang, Jonathan Tischler, Professor Vladimir Bulović

Vacuum growth of organic materials can generate atomically flat thin films of high purity, facilitating fabrication of complex multi-layer devices with excellent uniformity and sharp interfaces between adjacent layers. Such vacuum grown devices are highly reproducible from run to run, and can have complex structures containing thin layers of precisely controlled composition. Increased control over the growth parameter is essential for the better performance devices. Additionally, flexibility of van der Waal bonds in the organic thin films facilitate their integration with both conventional technologies and less conventional materials such as flexible, self-assembled, or conformable substrates.

We are in the process of developing a versatile materials growth system (see Fig. 1) that combines conventional materials growth techniques with novel deposition methods developed in our laboratories. The completed growth system will integrate the method for physical and vapor phase deposition of hybrid organic/inorganic thin-films with a low-pressure RF/DC sputtering chamber, an evaporative growth chamber, and a chemical vapor deposition chamber. The completed vacuum system will be capable of depositing molecular organics, polymers, metals, metal oxides, inorganic nanodots, and colloids in a controlled layer-by-layer fashion. An in-situ shadow masking system will enable fabrication of complex patterned structures inside a vacuum environment, while the integrated N_2-filled, dry glove box will facilitate handling, measuring, and packaging of organic thin film samples that are susceptible to reactions with atmospheric oxygen and water vapor. Completed samples will be in-situ tested in the analysis chamber by contacting them with an electrical probe attached to an X-Y-Z manipulator. Optical ports on the chamber allow for a telescopic view of the devices and facilitate optical excitation of probed samples. Optoelectronic properties of the hybrid materials and structures will be investigated at a range of temperatures form 5 K to 600 K, generated by the liquid helium cryostat and the boron-nitride heater situated behind the sample stage. The modularly attached AFM/STM chamber will facilitate in-situ atomic scale microscopy for evaluating morphology and electronic properties of hybrid materials.

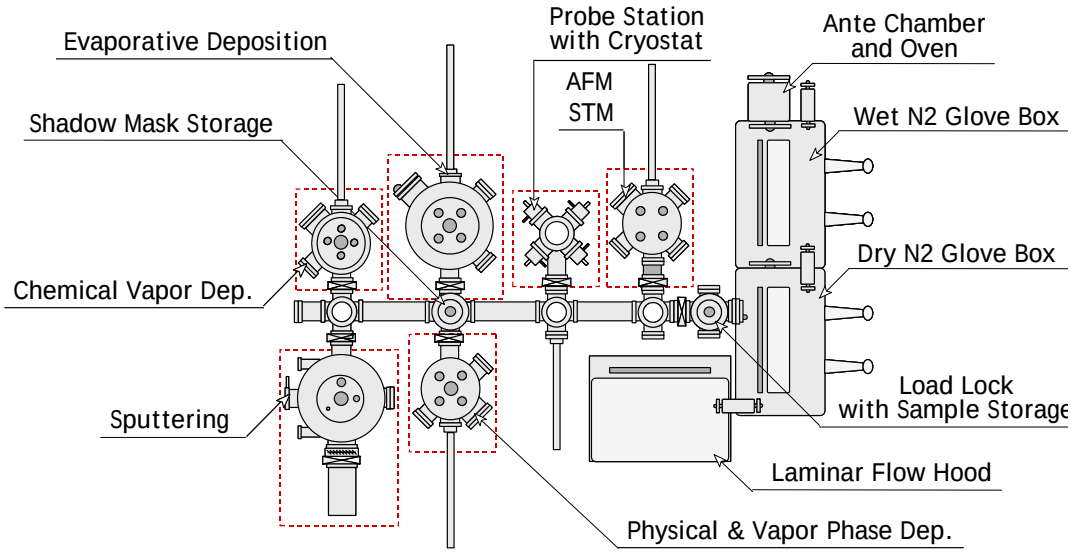

FIGURE 1 *Integrated materials and devices growth system consisting of the materials growth chambers based on physical and vapor phase deposition, sputtering, chemical vapor deposition, and evaporative deposition with in-situ shadow masking. Samples are analyzed in the analytical and AFM/STM chambers, and all connected to the central transfer line with load lock and an integrated, nitrogen-filled glove box.*

All chambers are connected to the central transfer system that has linear degrees of freedom. Maximum substrate size is 10 cm with a 5% variation in the thickness and composition of deposited films over the substrate area. The integrated growth system is the centerpiece of our materials growth effort, as in its completed form it will accommodate solvent-free deposition and co-deposition of polymers, colloids, and molecular organic materials in vacuum.

Solid State Solvation Effect

SPONSOR

National Science Foundation CAREER Award
National Defense Science and Engineering Graduate Fellowship – Department of Defense

PROJECT STAFF

Conor Madigan, Professor Vladimir Bulović

Emission and absorption spectra of many organic dyes in *liquid solutions* depend on the local electric fields generated by the surrounding polar solvent molecules. This "solvation effect" is a result of intermolecular solute-solvent interaction forces (such as dipole-dipole or dipole-induced dipole) that tend to stretch molecular bonds and shift charge distribution on molecules, altering the energy difference between the ground and excited states of the solute. Our experiments confirmed that the solvation effect is also present in *molecular solids* where closely packed polar molecules can generate large local electric fields. In the following two studies we develop a theoretical framework describing the effect.

Influence of Local Electric Fields on the Exciton Behavior in Amorphous Organic Thin Films

Performance of active organic opto-electronic devices is governed by the energy band structure of constituent thin films. In this project we examine the changes in the energy structure of amorphous molecular organic thing films due to local fields. Our goal is to develop a method for better predicting and ultimately fine-tuning the energy levels of such materials.

This work has grown out of two recent reports by our group [Bulović *et al.*, Chem. Phys. Lett. 287, 455 (1998) and 308, 317 (1999)] describing red shifts in the emission spectrum of amorphous organic thin films doped with the red laser dye DCM2 (chemical structures of materials used in this project are shown in Fig. 2). In these reports it was shown that by changing the concentration of DCM present in a film of N,N'-diphenyl-N,N'-bis(3-methylphenyl)-[1,1'-biphenyl]-4,4'-diamine (TPD) from 0.9% to 11%, the peak luminescence wavelength was shifted from λ=570 nm to λ=645 nm. Because DCM2 dye is highly polar (with a dipole moment μ~11D in the ground state) and TPD is a nonpolar molecule, increasing the dye concentration should enhance the local electric fields present in the film. The increase in the local fields is expected to shift the energy structure of polar DCM molecules resulting in the observed spectral shift.

A subsequent report by Baldo, *et al.* [Chem. Phys. Lett. 347, 297 (2001)] argued that the spectral shift is actually due to a progressive increase in the presence of aggregated dye molecules with increasing dye concentration, rather than the enhancement in the local fields. These authors posit that the emission of aggregate dye molecules is red-shifted and of similar efficiency to the emission of monomer dye molecules resulting in an overall luminescence red-shift at higher dye concentrations. We set out to clarify this issue, by developing experiments to distinguish between these two models, with the express purpose of generating a full-description of this solid-state solvation effect.

Photoluminescence measurements were performed on films consisting of a polystyrene (PS) matrix doped with a trace concentration of DCM2 laser dye, and between 0% and 35% by weight of the polar camphoric anhydride (CA) molecules. Upon excitation by λ=480 nm light only the fluorescence of DCM2 molecules was observed. This system allows us to keep the DCM2 concentration constant, and thereby fix DCM2 aggregation effects, while still modifying the local fields in the film by changing the

concentration of CA. The polymer host material polystyrene was chosen because it provides a non-polar background for the system. The polar camphoric anhydride was chosen because is has a large dipole moment (μ~6D in ground state) with a low molecular weight, and it is essentially optically inactive over the range of wavelengths relevant for studying the properties of DCM2.

For a fixed DCM2 concentration of < 0.005%, the DCM2 emission spectrum shifts continuously from 2.197 eV (565.0 nm) to 2.016 eV (615.5 nm) for CA concentrations ranging from 0% to 35% (see Fig. 2). These results show that large shifts in emission spectra can be observed in films that have negligible DCM2 aggregation. Furthermore, the spectral shift is correlated with the increase in the concentration of polar molecules in the amorphous host thin film. Assuming minimal CA:DCM2 aggregation, these results are consistent with the local-field-induced shifts proposed by Bulović *et al.*

The Bulović *et al.* study, however, gives no detailed description of the physical mechanism for the spectral shifts, leaving it unclear whether the shifts are due to static fields in the material, leading to a built-in Stark effect, or if they are due to dynamic relaxations in the material, leading to a solvatochromic shift as observed in liquids. By comparing emission *and* absorption spectra of PS:CA:DCM2 films, we are able to identify the extent to which static fields and dynamic relaxations are separately contributing. Surprisingly, initial measurements indicate that the spectral shifts follow the predictions of the solvation theory (although contributions from a static field could still be present).

Although further experiments must be performed, our present understanding is that the static fields in the doped films are the result of the arrangement of CA molecules around each DCM2 molecule during the formation of the film. Depending on the precise conditions under which the film forms, the extent to which this relaxation can proceed may change. For instance, if an arbitrary film is formed very rapidly and its constituent molecules afforded very little excess energy, it may be possible to entirely eliminate spatial correlation between molecules. On the other hand, annealing films after growth, or growing films very slowly, might enhance this spatial correlation. We expect that further study of this effect will provide considerable insight into the extent over which we can control molecular energy level structure by modifying the surrounding medium.

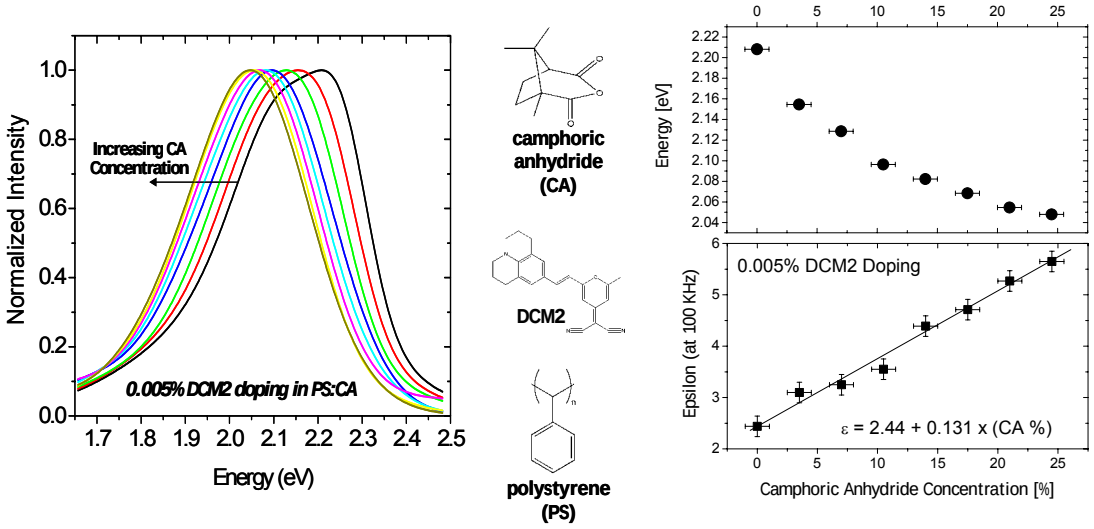

FIGURE 2 *(left) PL spectra of 0.005% DCM2 in PS:CA films. The spectrum red-shifts as the CA concentration is changed from 0 to 25%. (middle) Chemical structures of CA, DCM2, and PS. (right) Change of the peak luminescence energy and the dielectric constant as a function of CA doping.*

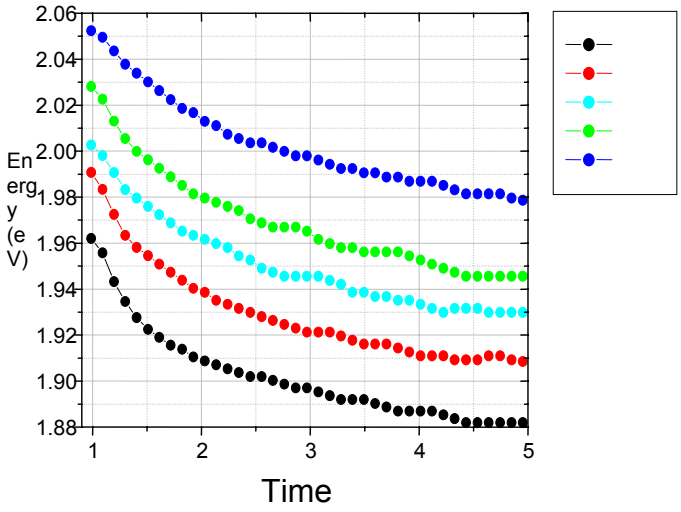

Figure 3 *(left) Spectral evolution of the PL spectrum of 4.7% DCM2 in Alq3 as a function of time after 100fs excitation with 400 nm light. (Inset) Schematic illustration of the experimental measurement. (right) Evolution of the peak of the photoluminescence spectra of Alq3:DCM2 films with different DCM2 concentrations (indicated in the plot).*

Exciton Diffusion and the Excitonic Density of States in Amorphous Organic Thin Film

In this project we investigate the process of exciton diffusion in amorphous organic thin films. As we will show below, the experimental observation of this process is integrally related to the excitonic density of states (DOS) in such films, and part of this project includes also the direct measurement of the DOS.

Numerous previous reports have established the importance of exciton diffusion by Forster energy transfer in amorphous organic thin films. For example, many groups studying organic light emitting diodes have demonstrated that excitons formed at a specific film interface can migrate significant

distances from that interface. While such diffusion can involve energy transfers between dissimilar molecules, the bulk of exciton diffusion occurs through Forster energy transfer between like molecules. The probability of exciton energy transfer is proportional to the overlap between the absorption spectrum of the final state and the emission spectrum of the initial state. An exciton is, therefore, far more likely to transfer from a higher energy site to a lower energy site than vice versa because the overlap between the respective emission and absorption spectra is larger in the former case. Consequently, diffusion by Forster energy transfer should progressively drive excitons towards the lowest energy sites in the system. The disorder in the amorphous neat films introduces a distribution of excitonic energies among different molecular sites, the lowest ones of which are preferentially occupied in the diffusion process.

The excition diffusion process can explain our recent observation of spectral shifts in the time resolved photoluminescence (PL) spectra of thin films of Alq_3 doped with the red laser dye DCM2 (Fig. 3). The films were excited by λ = 400 nm 100 fs pulses, and the signal was detected with a Hamamatsu Streak Camera with a maximum time resolution of 2 ps. In these measurements, we found that the PL spectra progressively red-shifted with time for the entire lifetime of the emission signal. For DCM2 doping levels of between 0.5% and 5%, we observed spectral shifts of more than 0.7 eV, with a small but continuous increase in the shift from lower to higher dopings (Fig. 3).

The spectral shifts are consistent with the exciton diffusion model. The smaller shifts observed for the samples with lower DCM2 concentration (larger DCM2 spacing) are consistent with the Forster energy transfer mechanism that is a very strong reciprocal function of distance (falling off as R^{-6}). We simulated numerically the diffusion process, starting with a large collection of spatially distributed DCM2 sites, with energies appropriate for the provided density of states (DOS). We then populate these sites with excitons, and allow them to either emit, or Forster energy transfer to another site during each time slice. The probabilities for these events are determined by supplied parameters. By tracking million excitons, we obtained smooth, repeatable ensemble PL spectra. In the course of these simulations, it became clear that given the “right” DOS function, we could very closely reproduce the observed experimental results (Fig. 4). However, so long as the DOS function remains a completely free parameter of the model, this remains a less than rigorous test of the theory.

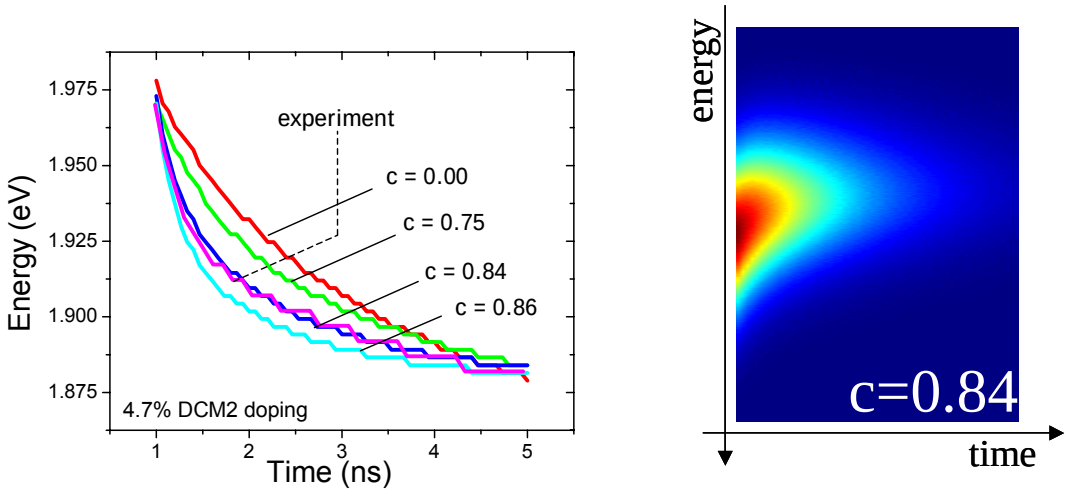

Figure 4 *(left) Comparison of the measured peak PL energy as a function of time, and the theoretical predictions based on the exciton diffusion model, for an Alq_3 film doped with 4.7% DCM2. The different values for c correspond to different density of states functions. Higher values of c indicate a narrower density of states, limiting at a delta function for c=1.0. For c=0, the density of states is simply the ensemble PL spectrum obtained immediately after the arrival of the laser pulse (i.e. before any diffusion occurs). (right) A PL intensity image of the emission spectrum as a function of time, produced by the simulator for the value of c best reproducing the experimental data. A spectral shift towards lower energies is observed.*

The DOS of DCM2 molecules in our films can be separately determined by employing single-molecule spectroscopy (SMS). We measure PL spectra of films with a low concentration of lumophores so that we can spatially resolve the individual molecules using a confocal microscope. The DOS of states so obtained is in a good agreement with the DOS predicted by our model.

Inorganic Quantum Dots in Organic Host Matrices for Efficient LEDs

SPONSOR

National Science Foundation MRSEC Program
Universal Display Corporation

PROJECT STAFF

Seth Coe, Wing Woo, Professor Moungi Bawendi, Professor Vladimir Bulović

Much effort has been devoted to improving the performance of organic light emitting devices (OLEDs) by increasing their efficiency, narrowing or broadening their emission spectra, or polarizing their emission. In this work we examine the benefits of incorporating other material systems within organic host matrices to generate efficient hybrid organic/inorganic LEDs of saturated color. Specifically, we describe OLEDs incorporating CdSe nanocrystallites, or quantum dots (QDs).

It has already been demonstrated that nanocrystallites of CdSe coated with a ZnS passivation layer have photoluminescence (PL) quantum efficiencies of as high as 50%, matching that of the best organic lumophores. By changing the diameter of the CdSe core from 23 to 55Å, the luminescence wavelength can be precisely tuned from λ = 470 nm to λ = 640 nm with a typical spectral full width at half of maximum (FWHM) of less than 40nm. The narrow FWHM of QDs results in saturated color emission. This leads to efficient QD-LEDs even in the red and blue parts of the spectrum, since in QD

emitting devices no photons are lost to infrared and UV emission. The broadly tunable, saturated color emission over the entire visible spectrum of a single material system is unmatched by any class of organic chromophores. Furthermore, environmental stability of covalently bonded inorganic nanocrystals suggests that device lifetimes of hybrid organic/inorganic LEDs should match or exceed that of all-organic LEDs, when nanodots are used as luminescent centers. The degeneracy of the band edge energy levels of QDs facilitates capture and radiative recombination of all possible excitons, whether generated by direct charge injection or energy transfer. The maximum theoretical QD-LED efficiencies are therefore comparable to the unity efficiency of phosphorescent OLEDs. The QD's excited state lifetime (τ) is much shorter ($\tau \approx$10ns) than a typical phosphor (τ>1μs), enabling QD-LEDs to operate efficiently even at high current density.

In this study, we incorporate inorganic quantum dots into electrically pumped molecular organic structures to prove their efficacy in OLEDs and examine the mechanisms of their electroluminescence (EL). Our basic device structure is shown in the inset of Fig.1, along with a schematic drawing of a core-shell type QD passivated with trioctylphosphine oxide (TOPO) caps. The QD solutions, prepared by the synthetic technique of Murray et al [C.B. Murray, *et al.*, J. Am. Chem. Soc. 115, 8706 (1993).], have emission spectra that peak at λ = 570nm, with an absorption maximum at λ = 559nm. The CdSe core diameter is approximately 38Å, and is overcoated with 1.5 monolayers of ZnS. The QDs are mixed in various concentrations into a chloroform solution of N, N'-diphenyl-N, N'-bis (3-methylphenyl)-(1,1'-biphenyl)-4,4'-diamine (TPD), which is then spin-cast onto clean, ITO coated glass substrates, resulting in a 40nm thick film. A 50nm thick film of tris- (8-hydroxyquinoline) aluminum (Alq_3) is then thermally evaporated onto the TPD:QD layer, and capped by a 1mm diameter, 75nm thick (10:1 by mass) Mg:Ag cathode with a 50nm Ag cap. The spin-casting and device manipulation during growth is performed in a dry nitrogen environment, with moisture and oxygen content of less than 5 ppm. All measurements are done in air.

The choice of organic host for the QDs is limited by material deposition methods. CdSe QDs are typically arranged into thin films by spin-casting from solution. While spin-casting is possible for molecular organics, and typical for polymer organics, it limits the available organic matrix materials to those that are highly soluble in solvents such as toluene, hexanes and chloroform, which are the preferred solvents for the TOPO capped QD colloids. In order to have a large range of possible solution mixtures and film thicknesses, it is necessary to have organic solubility in the range of 10mg/mL. Such is the case for TPD in chloroform. TPD has the added advantage of being a blue emitting material, which can facilitate access to the entire visible spectrum by doping different sized QDs into this organic matrix.

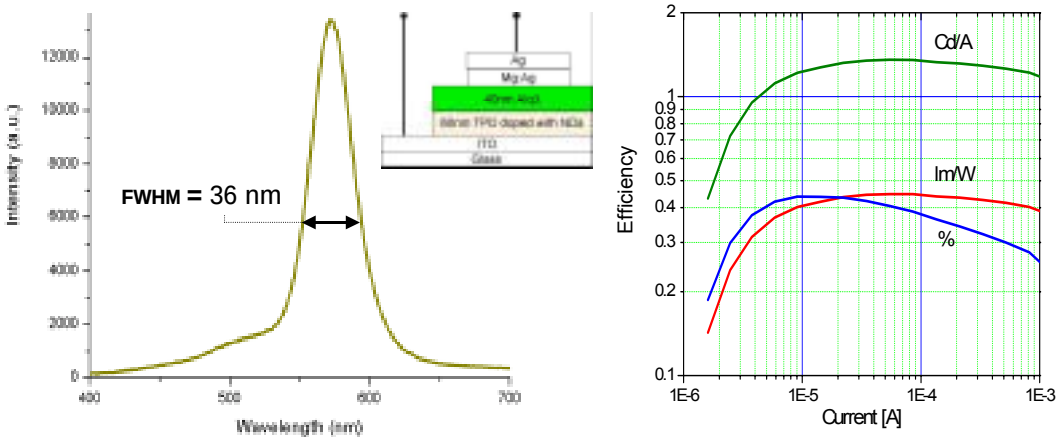

Figure 5 *Hybrid organic/inorganic light emitting device (HOI-LED). (Inset) HOI-LED cross section. (left) Electroluminescence spectrum at ~100 cd/m^2. (right) HOI-LED quantum efficiency in percent units, and luminescence efficiency in units of Cd/A and lm/W.reproducing the experimental data. A spectral shift towards lower energies is observed.*

A typical QD-LED emission is shown in Fig.5. The spectral peak at 570nm is due to the QDs, and the broader shoulder centered at 530nm we attribute to Alq_3 emission. The external quantum efficiency of QD-LEDs as a function of current is also shown in Fig.5, with the current-voltage plot for the same device shown in the inset. The peak quantum efficiency is 0.45% at 7mA/cm^2. At 125mA/cm^2, the LED luminance is 1500cd/m^2, which corresponds to a luminescence efficiency of 1.2 cd/A. This is a 20 fold improvement over the best previously reported QD-LED result [M. C. Schlamp *et al.*, J. Appl. Phys. 82, 5837 (1997).]. Device yields over hundreds of devices are greater than 90%, indicating a robust material system.

The spectrum and efficiency of QD-LEDs strongly depends on QD concentration in the TPD matrix. For low concentrations of QDs the device behavior is similar to an undoped structure, and at extremely high QD concentrations we observe a morphology change in the QD doped layer that leads to poor device performance and low yields. The thickness of the TPD:QD layer also plays a critical role in determining the device properties. With a thick TPD:QD layer, the Alq_3 emission is completely suppressed at the expense of lower quantum efficiency and higher turn-on voltage of the device. Thinning this layer leads to an excess of hole injection, and thus enhanced Alq_3 emission.

The observed spectra also show a minimal dependence on current density. Deep trap emission from the QDs is always present as a weak EL tail red-shifted from the main emission peak, but it saturates at very low currents (<1mA/cm^2). This deep trap emission is enhanced when incorporating core only QDs, rather than the core-shell type QDs utilized in our best devices. With the less stable QDs, the deep trap emission saturates at much higher current densities (~100mA/cm^2), resulting in LEDs with significant emission in the infrared. For optimum visible LED performance the overcoated dots are clearly preferred, though this observation may prove important as a means of characterizing the relative density of deep trap versus core level states.

The fundamental limits of QD-LED performance are significantly different than those of OLEDs. Our QD-LEDs have an emission FWHM of 36nm. In contrast, typical molecular organic LEDs have a FWHM of between 60 and 100nm, although emission of some polymers and phosphorescent molecules was shown to be as narrow as 26nm FWHM. However, in all of these cases the fundamental limit on bandwidth has already been achieved through materials preparation and purification. The vibrational structure of sterically flexible organics typically generates broad single molecule emission spectra at room temperature. The same is not true of the rigid, covalently bonded inorganic QD, for which single QD spectroscopy shows that the fundamental FWHM linewidth of a QD at room temperature is 14nm.

It is the combination of spectral diffusion and size distribution of QDs in a sample that yields further line broadening. Consequently, our 36nm linewidth corresponds to a size distribution of about 5%. It is reasonable to expect that new techniques in QD preparation and processing could lead to narrower QD-LED line widths. This true color saturation would be ideal for many applications where efficient production of narrowband light is desired. In particular, the creation of a high luminescent efficiency red LED requires both high external quantum efficiency as well as narrowband emission, to prevent the bulk of emission from occurring in the infrared where our eyes have minimal response. The deep trap emission that is typical of QDs could be problematic in achieving this goal, but the devices reported here already show less than 1% of their total power emitted in the infrared. This deep trap emission saturates at very low current densities. The spectral FWHM reported here is already an improvement over conventional OLEDs, and yet the fundamental limit has not been attained.

Smart Active-Matrix Display Drivers For Organic Light Emitting Devices

SPONSOR

MARCO Focused Research Center on Circuits and Systems

PROJECT STAFF

Eko Lisuwandi, Criswell Choi, Professor Charles Sodini, Professor Vladimir Bulović

In this project we are developing pixilated active matrix “smart drivers” for displays consisting of organic light emitting devices (OLEDs). Organic LEDs are perhaps the most promising novel technology for development of efficient, pixilated, and brightly emissive, flat-panel displays. They naturally emit over large areas, and offer the advantage of growth on lightweight and rugged substrates such as metal foils and plastic, with no requirement for lattice-matching.

Organic LED devices, however, exhibit non-liner light output responses that complicate their implementation in an application requiring a fine control of the output light intensity. Specifically, the I-V characteristics of OLEDs depend on the cathode/anode type, device layer thickness, and operating temperature. The power efficiency of pixels in a display will drift over time due operational degradation. The individual pixels in a display can then exhibit different aging, in accordance with their use. The brightness non-uniformities due to the differential aging will reduce the useful display lifetime.

Our smart active matrix circuitry compensates for the OLED non-uniformities by monitoring light output and adjusting the driving conditions according to the OLED performance. The adjusted output provides a defect-free picture. In the final design a Si *p-n* detector integrated behind each pixel will give feedback to the driver circuits that will adjust the proper current level to derive a constant brightness output. Figure 5 shows a typical integrated structure in which our patented transparent OLED is used. In this design both OLED electrodes are capable of transmitting the emitted light, which is mostly observed on the top, but is also partially absorbed in the detector.

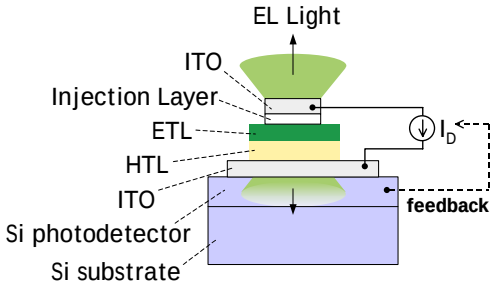

FIGURE 5 *An OLED pixel integrated with a "smart" Si active matrix driver. The Si photodetector monitors the intensity of the OLED pixel during the on state and provides feedback to the driving circuit to keep the light output intensity constant as the device efficiency changes with operation.*

The initial demonstration of the concept uses discrete components assembled on a PC board according to the 5 x 5 pixel array design scheme drawn in Fig. 6. Notice that three integrated transistors control each pixel. Also, each column of 5 pixels shares one feedback circuitry. The integrator type of compensation is used for each feedback circuitry to ensure that the light output is matched to the reference input. The values of discrete components were so chosen to stabilize the feedback loop.

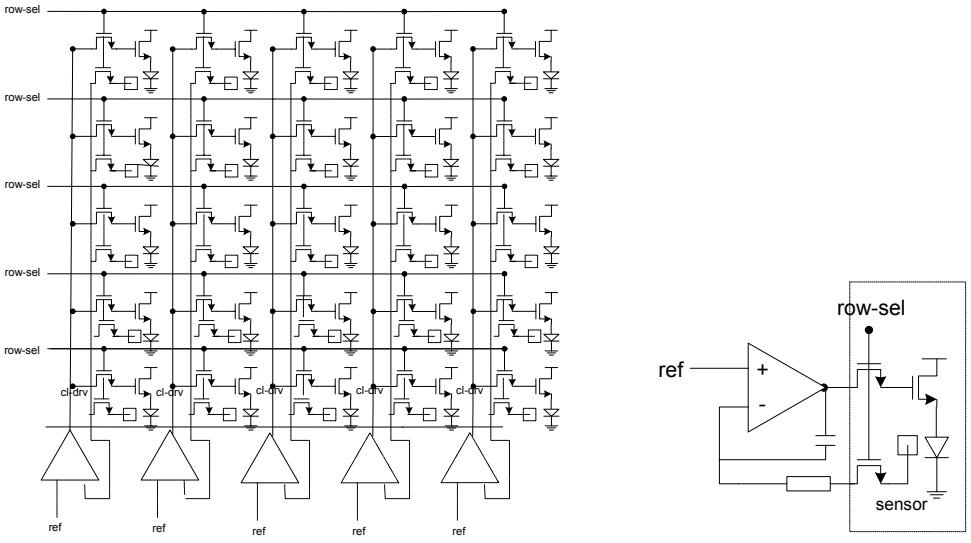

FIGURE 6 *(Left) A 5 x 5 pixel driver array with feedback. (Right) A single pixel detail.*

In our initial demonstration we use a digital video camera to serve the function of the integrated sensor. The digital part of the system and the image processing from the camera is done on a CPLD.

Figure 7 demonstrates the performance of the feedback loop on a 5 x 5 array powering LEDs. First, the LED array was intentionally set non-uniform (by adding series resistance to each pixel) before the feedback is done on the array. After the circuit executes the feedback the 5x5 array shows uniform brightness for all pixels.

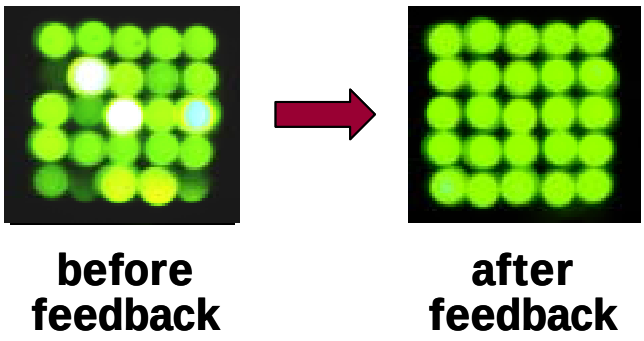

FIGURE 7 *(Left) Before feedback pixels were set intentionally non-uniform by addind/reducing serial resistance. (Right) After feedback the circuit reduces the current through the pixel in order to generate uniform pixel output.*

The next step of this project will include optimization of the feedback circuit to reduce the row-to-row output flicker, integration of the discrete circuit with standard OLED display, and finally moving the system onto a PCB. The steps beyond these will involve developing a functioning circuitry in crystal silicon and integrating the circuits with transparent OLEDs. We can then explore the implementation of the same circuit on flexible substrates using low-cost semiconductors (such as amorphous Si, or printed organic transistors).

Nanopattern-Assisted Growth of Organic Materials for Device Applications

SPONSOR

MARCO Focused Research Center on Materials, Structures, and Devices

PROJECT STAFF

Debbie Mascaro, Seth Coe, Nathan Lovell, Professor Vladimir Bulović

The goal of this work is to use nanopatterning to improve the performance of organic optoelectronic and electronic devices such as organic light emitting diodes (OLEDs) and organic field effect transistors (OFETs). OLEDs and OFETs are devices in which thin films of organic small molecules serve as light emitting or charge transporting materials. The organic thin films are typically prepared by thermal evaporation onto unpatterned SiO_2 or indium tin oxide (ITO)-coated SiO_2 substrates. We have evaporated organic materials onto nanopatterned substrates in order to (1) improve light extraction from OLEDs and (2) promote molecular ordering in OFET thin films. The nanopatterning is accomplished by interference lithography, and results in features that are on the order of hundreds of nanometers in size.

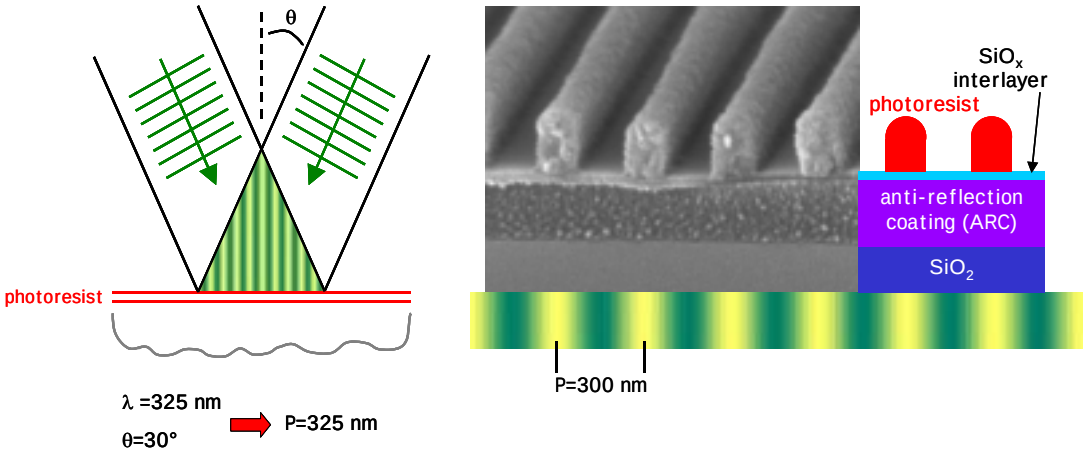

FIGURE 8 *Schematic representation of the interference lithography process (left) and its application to generating a periodic pattern in the photoresist layer (right).*

Nanopatterning by Interference Lithography

In interference lithography, photoresist is exposed by the optical standing wave generated by the interference of two coherent beams of light. For a single exposure, the resulting pattern is a linear grating as shown in Fig. 8. The grating period (P) is determined both by the wavelength (λ) of light used and by the angle (θ) of the beam with respect to the substrate normal, and is given by $P = \lambda / 2 \sin \theta$. Typically a trilayer resist stack is used, which consists of an anti-reflection coating (ARC) to prevent back reflections from the Si substrate, an SiO_x interlayer to serve as an etch mask, and finally the photoresist (see Fig. 8).

For this work, all interference lithography was performed in the Nanostructures Laboratory (NSL) at MIT using a Lloyd's Mirror configuration. In this configuration, part of the light from a HeCd laser (λ=325 nm) is directly incident on the substrate while part of the light is reflected onto the substrate by a mirror oriented perpendicular to the substrate. Accessible periods using this setup are 170 nm up to 1 μm.

After two exposures, with the substrate rotated by some angle for the second exposure, we can generate a two dimensional pattern. For a 90 degree rotation the resulting pattern is a square array of posts or holes if positive or negative resist is used, respectively. The typical dose used for the each of the two exposures is 65 percent of that needed to clear the resist in a single exposure. Figure 9 show SEM micrographs of a square array of posts in a positive photoresist. When the substrate is rotated by 60 degrees for the second exposure, a hexagonal pattern is generated.

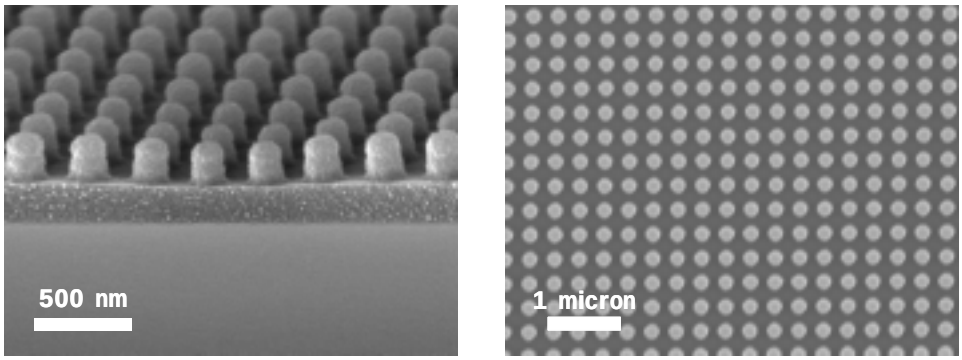

FIGURE 9 *Photoresist pillars generated after two exposures of the photoresist to the light interference pattern.*

Application of Nanopatterning to Organic Light Emitting Devices -Light Extraction

A typical OLED is fabricated by first evaporating organic layers on top of an ITO-coated glass substrate, and then evaporating a metal cathode on top of the organic layers. The weak microcavity that is formed by the reflective electrode and reflection at the glass/ITO interface can sustain highly-lossy waiveguided modes. The waveguided light dissipates most of its energy to the metal electrode after a very short propagation (sub-micron path length). Furthermore, light in the radiative modes of the OLED, emitted at shallow angles can also be absorbed by the structure after multiple total internal reflections. Such losses in OLED efficiency can account for more than 60% of all the internally generated radiation. In order to improve the OLED efficiency it is, therefore, desirable to devise a device structure that redirects the light into vertically-emitted radiative modes.

Following earlier studies in III-V materials we propose to redirect the in-plane-emitted light by incorporating a two-dimensional photonic band gap (PBG) structure into the design of our OLED active layers. One possible PBG structure is simply a hexagonal lattice of air holes in a high-dielectric semiconductor. By varying the period and size of the PBG features, or the index of the semiconducting material, this design can be tuned to prevent in-plane propagation of a specific band of emission wavelengths.

We generated a PBG structure in PDMS (silicone rubber) substrates by making a “master” in a photoresist layer on Si and then transferring that pattern to PDMS (see Fig. 10). Top view SEM micrographs of a PDMS stamp made from a square lattice of posts are also shown in Figs. 10a and 10b. The period was 340 nm, and the thickness of the photoresist was 200 nm, resulting in 200 nm deep holes in the PDMS. In the final processing step we evaporated a 100 nm thick luminescent organic layer of TPD on top of our PDMS stamp.

We investigated photoluminescence of the TPD film (peak luminescence wavelength, λ_{max}= 415 nm) excited by a mm^2 beam of UV light. We observed directed in-plane guiding of light, consistent with the square pattern of the PBG structure (Fig. 10c). This initial study demonstrates the effectiveness of PBG structures in redirecting luminescence in organic devices. In the next step we will use the same method to fabricate PBG patterns in active OLED structures.

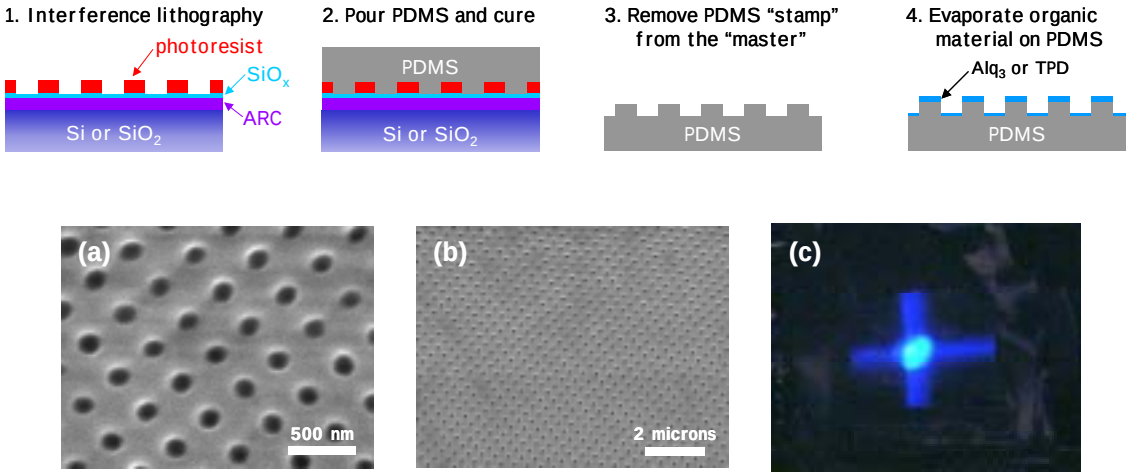

FIGURE 10 *(top) Sequence of steps for generating a PDMS PBG structure with an organic luminescent layer on top. (a) and (b) Different magnifications of the patterned PDMS structure. (c) Directionally guided light in a cm^2 PDMS substrate. The excitation beam impinges the substrate at the bright center spot.*

Application of Nanopatterning to Organic Field Effect Transistors - Molecular Ordering

Unlike the amorphous organic films used in OLEDs, organic thin films used in organic FETs are typically polycrystalline. As in a conventional FET, the amount of current that flows between the source and the drain electrodes is modulated by the field applied across the metal (gate)-insulator-semiconductor sandwich. The charge carrier mobility through the organic thin film is strongly dependent on the molecular ordering within the film, where the mobilities can be as much as eight orders of magnitude larger for single-phase polycrystalline films as compared with amorphous films of the same material. Our goal is to improve molecular ordering within polycrystalline organic films in order to achieve larger grain sizes and lower defect densities, and ultimately enhance the charge carrier mobility.

A common approach to improving molecular ordering is by modifying the insulating surface onto which the organic semiconductor is deposited. For example, SiO_2 can be treated with silanes such as octadecyltrichlorosilane to create a hydrophobic self-assembled monolayer (SAM). Mechanical modification, such as rubbing a polymeric insulator or a thin pre-film of the organic semiconductor itself, is another possibility. Our approach is similar to this mechanical modification, but more controlled. We use interference lithography to pattern surface relief gratings into an SiO_2 substrate, and then evaporate an organic semiconductor such as pentacene onto this substrate. We expect to observe either graphoepitaxy, by which the molecules are aligned by the artificial surface pattern, or confinement effects, by which defects segregate to the boundaries of the confined grains.

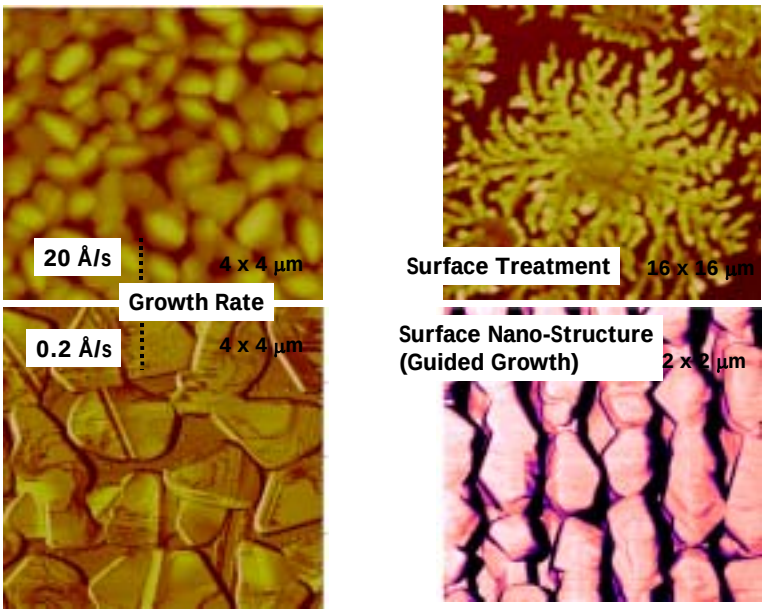

FIGURE 11 *Effects of growth rate, surface treatment, and nano-patterns on the growth of tetracene thin films.*

Our initial investigations of deposited film morphology have been done using both scanning electron microscopy (SEM) and atomic force microscopy (AFM). Figure 11 shows the morphology of four tetracene thin films grown on differently treated SiO_2 substrates. For all films the deposition pressure was 5 x 10^{-6} Torr, and the substrate was held at room temperature during deposition. Both surface treatment and the growth rate are seen to strongly influence the morphology of films. Significant order is observed for the nano-patterned substrates, where the grains on the plateaus appear to be larger for the deeper gratings. At this time we are also pursuing electron diffraction, x-ray diffraction and polarized fluorescence microscopy measurements in order to further understand the effect of the gratings on the molecular order within the film.